Metab Brain Dis (2010) 25:49–56
DOI 10.1007/s11011-010-9181-2

ORIGINAL PAPER

Human ^{13}N-ammonia PET studies: the importance of measuring ^{13}N-ammonia metabolites in blood

Susanne Keiding · Michael Sørensen · Ole Lajord Munk · Dirk Bender

Received: 27 August 2009 / Accepted: 28 January 2010 / Published online: 9 March 2010

Abstract Dynamic ^{13}N-ammonia PET is used to assess ammonia metabolism in brain, liver and muscle based on kinetic modeling of metabolic pathways, using arterial blood ^{13}N-ammonia as input function. Rosenspire et al. (1990) introduced a solid phase extraction procedure for fractionation of ^{13}N-content in blood into ^{13}N-ammonia, ^{13}N-urea, ^{13}N-glutamine and ^{13}N-glutamate. Due to a radioactive half-life for ^{13}N of 10 min, the procedure is not suitable for blood samples taken beyond 5–7 min after tracer injection. By modifying Rosenspire's method, we established a method enabling analysis of up to 10 blood samples in the course of 30 min. The modified procedure was validated by HPLC and by 30-min reproducibility studies in humans examined by duplicate ^{13}N-ammonia injections with a 60-min interval. Blood data from a ^{13}N-ammonia brain PET study (from Keiding et al. 2006) showed: (1) time courses of ^{13}N-ammonia fractions could be described adequately by double exponential functions; (2) metabolic conversion of ^{13}N-ammonia to ^{13}N-metabolites were in the order: healthy subjects > cirrhotic patients without HE > cirrhotic patients with HE; (3) kinetics of initial tracer distribution in tissue can be assessed by using total ^{13}N-concentration in blood as input function, whereas assessment of metabolic processes requires ^{13}N-ammonia measurements.

In this paper, the term ammonia refers to the sum of unionized NH_3 and ionized NH_4^+

S. Keiding (✉) · M. Sørensen · O. L. Munk · D. Bender
PET Centre, Aarhus University Hospital,
Aarhus 8000, Denmark
e-mail: susanne@pet.auh.dk
URL: www.liver.dk

S. Keiding · M. Sørensen
Department of Medicine V (Hepatology),
Aarhus University Hospital,
Aarhus, Denmark

Keywords ^{13}N-ammonia metabolism · Positron emission tomography · Ammonia metabolites · Solid-phase extraction · Brain PET

Introduction

Hepatic encephalopathy (HE) is a severe neurological condition arising secondary to liver failure. Hyperammonemia is considered a major causative factor because most patients with HE have elevated blood concentrations of ammonia, which in high concentrations is neurotoxic (Cooper and Plum 1987; Jones and Basile 1998; Cooper 2001; Butterworth 2002: Johansen et al. 2007; Iversen et al. 2009). Dynamic ^{13}N-ammonia PET has been used in humans to assess ammonia metabolism in brain (Lockwood et al. 1979, 1984, 1991; Ahl et al. 2004; Weissenborn et al. 2004; Keiding et al. 2006; Sørensen and Keiding 2007a; Sørensen et al. 2009; Berding et al. 2009), liver (Keiding et al. 2001, 2005; Sørensen and Keiding 2007b) and muscle (Nishiguchi et al. 2003). The PET procedure encompasses intravenous injection of ^{13}N-ammonia tracer followed by dynamic measurements of radioactivity concentrations in arterial blood (samples) and tissue (PET camera). Data are analyzed by fitting kinetic models of the metabolic pathways to the time courses of the tissue radioactivity concentrations, using the time course of radioactivity concentrations in blood as input function. However, appearance of ^{13}N-urea, ^{13}N-glutamine and other ^{13}N-labelled amino acids in blood (Cooper et al. 1979; Lockwood et al. 1979; Nieves et al. 1986; Rosenspire et al. 1990; Keiding et al. 2006) complicates the kinetic analysis. Consequently the analysis of dynamic ^{13}N-ammonia PET studies is sometimes limited to assessment of distribution and transport processes across the plasma membrane during the very first minutes after

tracer injection, using total ^{13}N-radioactivity concentration in blood as input function (Ahl et al. 2004). In agreement with this, we showed that formation of ^{13}N-metabolites can be ignored for the assessment of the initial distribution of tracer (Sørensen and Keiding 2006). However, calculation of parameters of steady-state metabolic processes requires the use of metabolite-corrected input functions, i.e. ^{13}N-ammonia concentrations (Keiding et al. 2006, Sørensen and Keiding 2006; Bass et al. 2009).

Various attempts have been made to fractionate unmetabolized ^{13}N-ammonia and ^{13}N-labelled metabolites in blood (Cooper et al. 1979; Lockwood et al. 1979; Nieves et al. 1986; Rosenspire et al. 1990). The most robust method was published by Rosenspire et al. (1990) who introduced a sequential solid phase extraction procedure which combines the use of cation and anion exchange resins, allowing for fractionation of the ^{13}N-content in blood into ^{13}N-acidic amino acids, ^{13}N-ammonia, ^{13}N-neutral amino acids, and ^{13}N-urea. However, only results from blood samples taken up to 5 min after injection of ^{13}N-ammonia in healthy human subjects were published (Rosenspire et al. 1990). Due to the radioactive half-life of ^{13}N-nitrogen of 10 min the method is not suitable for blood samples taken beyond 5–7 min after injection of the ^{13}N-ammonia tracer. By modifying Rosenspire's method, we established a method which enables us to analyze up to 10 blood samples in the course of a 30-min dynamic human ^{13}N-ammonia PET study (Keiding et al. 2006). In the present study we describe our technical modifications of Rosenspire's method and give detailed reports of the ^{13}N-metabolite measurements in Keiding et al. (2006), including validation by means of radio-HPLC measurements and studies of reproducibility in 30-min studies of human subjects who were given two successive ^{13}N-ammonia injections.

Material and methods

Human subjects

The method was used to determine ^{13}N-metabolites in blood samples in a brain PET study of 5 healthy subjects, 8 cirrhotic patients with type C HE, and 7 cirrhotic patients with neither overt, nor minimal HE (Keiding et al. (2006) and here we give a detailed report of the technical procedure and the ^{13}N-metabolite measurements. Data from another five patients with compensated liver cirrhosis who were given two injections of ^{13}N-ammonia at a 60-min interval are also included.

^{13}N-ammonia was produced at the radiochemistry facility of the PET Centre, Aarhus University Hospital, with a radiochemical purity >98% and a specific radioactivity of 30–40 GBq/μmol. 500 MBq ^{13}N-ammonia was injected intravenously over 15 s, and arterial blood samples were collected via a small catheter placed in a radial artery (Artflon Becton Dickinson, Swindon, UK) in heparinized 1.5 ml Eppendorf tubes after 1, 2, 3, 5, 7, 10, 15, 20, 25, and 30 min.

All studies were approved by the Ethics Committee of Aarhus County, and informed consent was obtained from each subject. No complications to the procedure were observed.

Preparation of solid phase extraction columns

Three columns for the sequential solid phase extraction procedure were prepared at the PET Centre. Plungers from 1 ml Tuberculin syringes (Codan Medical Aps, Rødby, Denmark) were removed, and quartz wool was put into the syringes to fix exchange resins in the syringes. The resins were conditioned immediately before each study. All chemicals for conditioning the ion exchange resins were purchased from Sigma-Aldrich Denmark, Vallensbæk Strand, Denmark. *Column 1:* Dowex 1X8–50 anion exchange resin, 20–50 mesh, chloride form was converted to the acetate form by flushing the resin with at least 10 volumes of 0.75 M sodium acetate trihydrate solution. 0.5–0.6 ml of this anion exchange resin in acetate form was manually filled in the 1 ml syringe. *Column 2:* AG 50 W-X8 resin hydrogen form 100–200 mesh (Bio-Rad Laboratories, Hercules, CA) was converted to tris(hydroxymethyl)aminomethane (TRIS) form by flushing the resin with at least 10 volumes of a solution prepared from 0.8 M solution of TRIS acetate (freshly prepared from equal molar amounts of TRIS and glacial acetic acid). 250–350 μL of this resin were manually filled in the 1 ml syringe. *Column 3:* AG 50 W-X8 resin hydrogen form 100–200 mesh (Bio-Rad Laboratories, Hercules, CA) was flushed with at least 10 volumes of Millipore water. 250–350 μL of this resin were manually filled in 1 ml syringes.

The employed Bio-Rad AG 50 W-X8 resin is chemically equivalent to the originally used Dowex 50(H^+) resin by Rosenspire et al. (1990).

The original method by Rosenspire et al. (1990) comprised elution of resin-bound radioactivity with 2 M potassium chloride solution for radioactivity measurements in a well counter. In our adaptation, the syringes, containing the resins and trapped ^{13}N-metabolites, were placed directly in the well counter.

Solid phase extraction procedure

A volume of 0.5 ml whole-blood was added to 0.5 ml of a 10 wt% solution of sulfosalicylic acid. After vigorous shaking, the samples were centrifuged for 2 min at 13,000 rpm to precipitate proteins. For solid phase extraction procedures, Alltech Visiprep® manifolds were

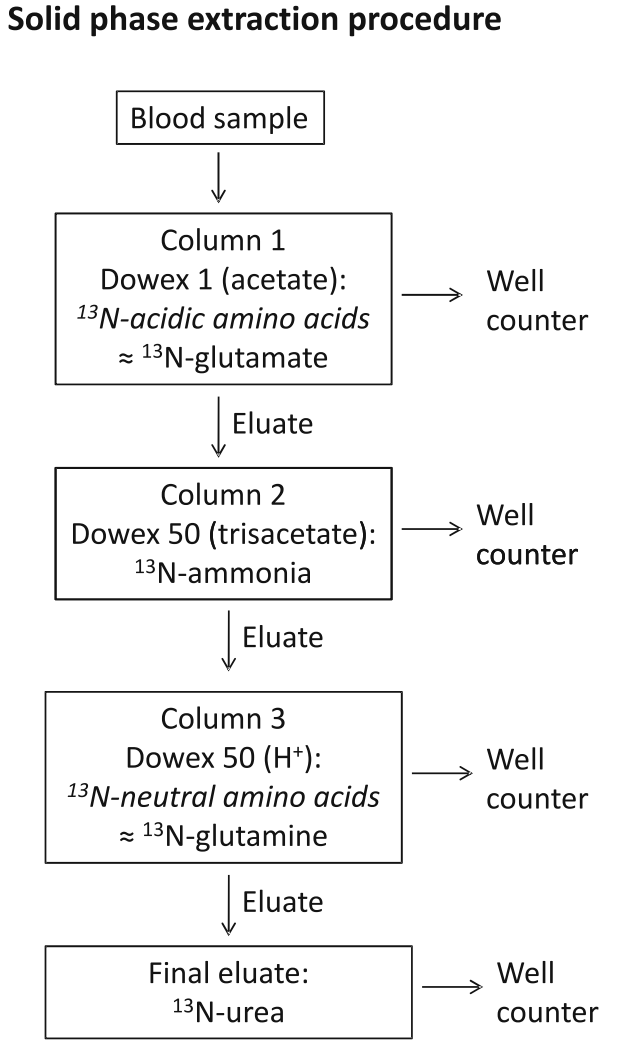

Fig. 1 Diagram of sequential solid phase fraction extraction procedure for determination of ^{13}N-metabolites

employed. As illustrated in Fig. 1, the supernatant from the worked-up blood sample was transferred on to *Column 1* containing the acetate-conditioned resin, followed by 5–10 s suction through the resin. The resin was washed with 4 ml of Millipore water. The column with resin-bound radioactivity was transferred into a counting tube and radioactivity was measured in a well counter (^{13}N-containing acidic amino acids; mainly ^{13}N-glutamate). The mixed eluate and Milipore water was then sucked through *Column 2*, containing TRIS-conditioned resin. The resin was washed with 2×3.5 ml Millipore water, and resin-bound radioactivity (^{13}N-ammonia) was measured in a well counter. The mixed eluate and Milipore water was sucked through *Column 3*, containing resin in hydrogen form. This resin was washed with 3×3.5 ml water and the resin-bound radioactivity counted in a well counter (^{13}N-labeled neutral amino acids; mainly ^{13}N-glutamine). According to Rosenspire et al. (1990), the radioactivity in the final washing solution is attributed to ^{13}N-urea. The solution (final eluate+Milipore water) was collected in a pre-weighed plastic beaker and 5 ml of the solution was counted in a well counter. The pre-weighed plastic beaker was weighed again, and the amount of radioactivity in the 5 ml solution was related to the entire final volume.

To ensure a high through-put of samples, we used 2 Visiprep manifolds simultaneously.

Counting statistics

Count rates were generally lower for blood samples taken at late time points than for blood samples taken earlier because of the radioactive half-life of 10 min resulting in less accurate counting statistics (Table 1). The measurement accuracy was slightly better for the first two fractions, i.e. for ^{13}N-glutamate and ^{13}N-ammonia than for the ^{13}N-glutamine and ^{13}N-urea fractions, probably due to adsorption of ^{13}N-substances to the plastic tubes during elution and transfer of the liquids (Fig. 1 and Table 1). Furthermore, the relative large measurement uncertainty for ^{13}N-urea may be explained by the poor counting statistics due to dilution of 0.5 ml blood to approximately 20 ml during the procedure and counting of only 5 ml of this solution in the well counter.

Rosenspire et al. (1990) also proposed a simplified solid phase extraction procedure, using separation into only two fractions, ^{13}N-ammonia and ^{13}N-metabolites. However, in our hands this procedure overestimated the ^{13}N-ammonia fraction because of insufficient removal of especially ^{13}N-urea.

Radio-HPLC

Radio-HPLC was used for validation of the solid phase extraction procedure. The radio-HPLC analysis of ^{13}N-ammonia and ^{13}N-metabolites was adopted from Nieves et al. (1986), using a cation exchange HPLC column with two

Table 1 Reproducibility of the modified sequential solid phase extraction procedure for measurement of ^{13}N-labelled metabolites in blood

	^{13}N-glutamate	^{13}N-ammonia	^{13}N-glutamine	^{13}N-urea
Coefficient of variation (%)	1.5 (0.1–7)	7.7 (0–28.9)	11.2 (0.1–42.5)	17.9 (0–57.3)

Data are shown as mean and range of coefficients of variation between two measurements of ^{13}N-fractions in blood samples taken 1–30 min after intravenous administration of 500 MBq ^{13}N-ammonia to 5 cirrhotic patients without HE (Fig. 2). For each metabolite the lowest value is from the 1-min time point and the highest value from the 30-min time point

different phosphate buffers. The time required for analyzing one blood sample was 25–30 min. Because of this and the physical half-life of ^{13}N of 10 min, we restricted the use of the radio-HPLC analysis to blood samples taken 5 and 15 min after tracer injection (from Keiding et al. 2006).

When compared to the radio-HPLC results, the solid phase extraction procedure yielded valid estimates of the individual ^{13}N-metabolite fractions.

Results and discussion

Reproducibility

The reproducibility study showed no significant difference between the two time courses of the ^{13}N-ammonia fractions for any of the 5 subjects (Fig. 2) or any of the other ^{13}N-fractions. Coefficients of variation for each of the four fractions indicate good reproducibility being best in the first minutes after the ^{13}N-ammonia tracer injection due to better counting statistics (Table 1). Overall, measurement accuracy was fine for the present purpose.

Time course of ^{13}N-metabolite fractions

The time courses of the ^{13}N-ammonia fractions after tracer injection in the three groups of human subjects in Keiding et al. (2006) are shown in Fig. 3 and typical examples of the time course of the ^{13}N-metabolite fractions in a cirrhotic patient with HE and a healthy subject are shown in Fig. 4 (from Keiding et al. 2006). ^{13}N-urea and ^{13}N-glutamine appeared at a slower rate in the cirrhotic patients than in the healthy subjects, as illustrated in Fig. 4. Both the ^{13}N-ammonia fractions and the ^{13}N-metabolite fractions had an initial time delay of a little less than 1 min. This can be ascribed to combined effects of blood circulation time and time delay for formation of ^{13}N-metabolites. The 30-min time courses of the ^{13}N-ammonia fractions were described adequately by double exponential curves with an initial time delay (Fig. 3 and Table 2). The decreasing ^{13}N-ammonia fraction was divided into of an initial fast component (A and α) and a final slow component

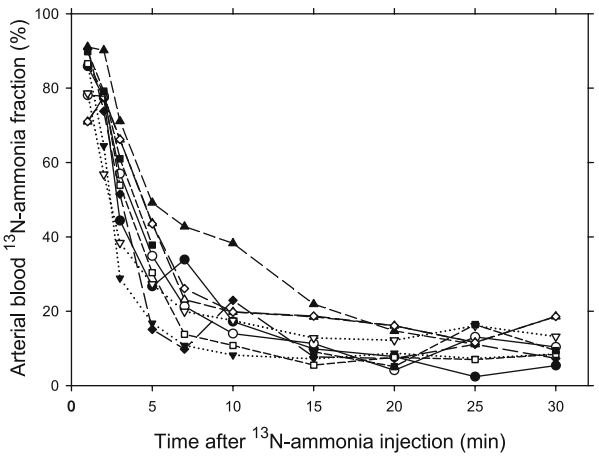

Fig. 2 Reproducibility study. Time courses of the ^{13}N-ammonia fractions in arterial blood in 5 cirrhotic patients without HE, each studied by two successive ^{13}N-ammonia injections with a 60-min interval. Data points from the two injections in a patient are shown by similar symbols, being open and closed, respectively, and points from each injection are connected by lines with the same type of line

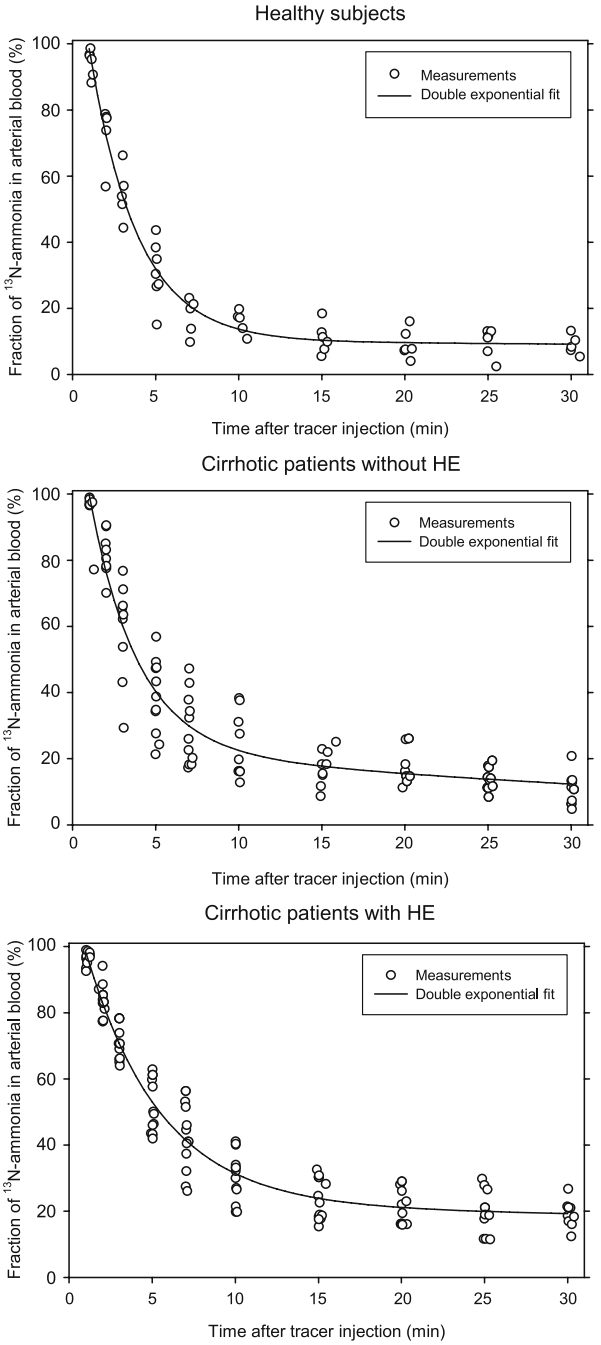

Fig. 3 Time course of fractions of ^{13}N-ammonia in arterial blood in three groups of subjects as indicated (from Keiding et al. 2006). Curves are double exponential fits (see Table 2)

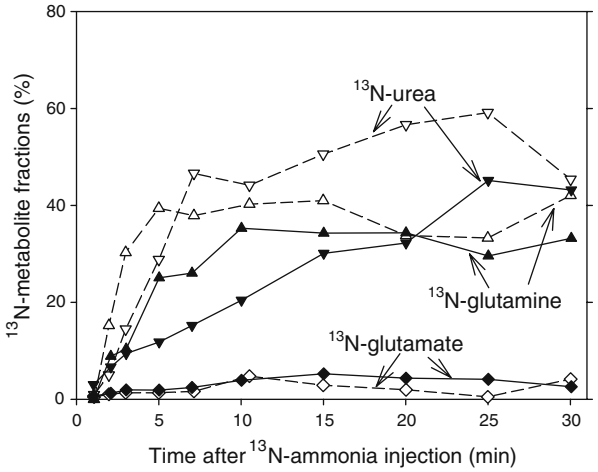

Fig. 4 Examples of ^{13}N-metabolite fractions in arterial blood in a cirrhotic patient with HE (closed symbols) and a healthy subject (open symbols)

((100%–A) and β) (Table 2). We ascribe the fast component as the result of metabolic conversion of the injected ^{13}N-ammonia into ^{13}N-metabolites, see also Fig. 4.

The metabolic conversion of ^{13}N-ammonia comprised a larger part in the group of healthy subjects (A=90%) than in the two groups of patients with cirrhosis (77% and 78%, respectively) and it was slower in the group of cirrhotic patients with HE (α, 0.22 min^{-1}) than in the two other groups of subjects (α, 0.35 min^{-1} in both groups) (Table 2). Overall the data thus indicate that the metabolic conversion of ammonia took place in the order: healthy subjects > cirrhotic patients without HE > cirrhotic patients with HE.

It is noticeably that the subsequent slow component does not approximate zero within the present 30-min study period. It is influenced not only by continued metabolic conversion of ^{13}N-ammonia, but also by formation of ^{13}N-ammonia from breakdown of ^{13}N-glutamine in muscle tissue (Duda and Handler 1958; Mobley and Hausinger 1989; Cooper 2001; Nishiguchi et al. 2003; Sørensen and Keiding 2006), breakdown of ^{13}N-urea by ureases in the intestines (Prior and Visek 1972; Hansen and Vilstrup 1985; Mobley and Hausinger 1989) and unequal volumes of distribution of the formed metabolites (Berl et al. 1962).

In our brain PET study we found that separate accounting for blood ^{13}N metabolites improved the goodness of the kinetic fitting as evaluated by residuals of the fits when compared with a model ignoring the time courses of the metabolites (Keiding et al. 2006).

Table 2 Parameters from fitting double exponential equations to the time courses of ^{13}N-ammonia fractions in arterial blood (from Keiding et al. 2006) following iv 500 MBq ^{13}N-ammonia tracer injection: ^{13}N-ammonia fraction = $Ae^{-\alpha(t-td)} + (100 - A)e^{-\beta(t-td)}$. The ^{13}N-ammonia fraction is 100% between t=0 and t=td

Parameter[a]	Healthy subjects	Cirrhotic patients without HE	Cirrhotic patients with HE
td (min)	0.95	0.99	0.91
A (%)	90	77	78
α (min^{-1})	0.35	0.35	0.22
β (min^{-1})	0.4 10^{-2}	2.2 10^{-2}	0.4 10^{-2}

[a] Double exponential equation: ^{13}N-ammonia fraction (%); t is time after tracer injection (min); td is time delay between tracer injection and appearance of ^{13}N-metabolites in blood (min); A and (100%–A) are the coefficients (%); α and β are exponents of the fast and slow components, respectively (min^{-1})

Time courses of ^{13}N-ammonia concentrations and body clearance of ^{13}N-ammonia

The time course of the ^{13}N-ammonia concentration in blood was calculated from the measured total ^{13}N-concentration (Fig. 5) and the ^{13}N-ammonia fractions (Fig. 4 and Table 2)

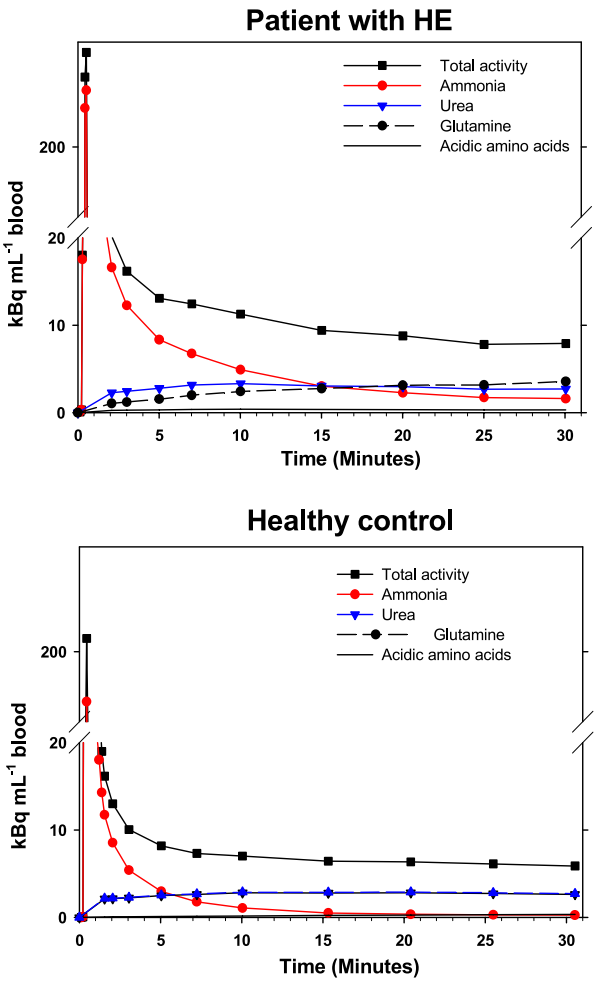

Fig. 5 Time-courses of blood concentrations of total ^{13}N-radioactivity concentrations (*black*) and of ^{13}N-ammonia (*red*) and ^{13}N-metabolites (*blue* and *black*) after intravenous injection of 500 MBq ^{13}N-ammonia tracer to a cirrhotic patient with HE (*upper graph*) and a healthy subject (*lower graph*). The time-courses of ^{13}N-urea and ^{13}N-glutamine are coincident in the healthy subject

in each subject. The time course of the blood concentration of ^{13}N-ammonia depends on ^{13}N-metabolite formation and distribution of ^{13}N-ammonia and ^{13}N-metabolites. In general, blood concentration of ^{13}N-ammonia decreased faster and to a lower level within the present experimental period the healthy subjects than in the patients with cirrhosis (Fig. 5 shows an example). We therefore tested the hypothesis that whole-body clearance of ammonia was decreased in the patients with cirrhosis (Sørensen and Keiding 2006). All subjects received the same dose of ^{13}N-ammonia tracer, and we therefore used the areas-under-the-curve of the ^{13}N-ammonia concentrations as approximate "inverse" estimates of whole-body clearance of ammonia (Fig. 6). It is seen that AUC was approximately the same in cirrhotic patients without HE and healthy subjects and that it was significantly higher in cirrhotic patients with HE than in the two other groups of subjects, meaning that the patients with HE had a lower body clearance than the two other groups of subjects. Taken together with the above analysis of the time course of the ^{13}N-ammonia fractions, the data strongly indicate that metabolic conversion of ammonia is reduced in patients with de-compensated cirrhosis (here HE).

The finding of a lower body clearance of ammonia cirrhotic patients with HE than cirrhotic patients without HE again underline the connection between blood ammonia and HE (Keiding et al. 2006; Iversen et al. 2009), especially because the uptake of ammonia into the brain is linearly correlated to the blood concentration of ammonia (Lockwood et al. 1979; Keiding et al. 2006).

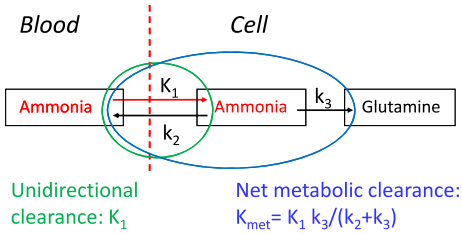

Fig. 7 Simplified diagram of ammonia metabolism in brain: K_1 is the unidirectional clearance of ^{13}N-ammonia from blood into cells (ml blood/min/ml tissue), K_{met} is the net metabolic clearance of ^{13}N-ammonia from blood into intracellular of ^{13}N-metabolites (ml blood/min/ml tissue), k_2 the rate constant for back-flux from cell to blood of un-metabolized ^{13}N-ammonia (min^{-1}), and k_3 the rate constant for conversion of ^{13}N-ammonia to ^{13}N-metabolites (min^{-1})

Cerebral ^{13}N-ammonia kinetics and blood-brain-barrier for ammonia

It has been argued that the initial brain ammonia PET kinetics can be analyzed adequately using total blood ^{13}N-concentrations without correction for ^{13}N-metabolites (Ahl et al. 2004). We tested this assumption by comparing the initial unidirectional clearance (K_1) using ^{13}N-ammonia concentration and total ^{13}N-concentration as input function, respectively, in a kinetic analysis according to the diagram of the metabolic processes shown in Fig. 7 (Sørensen and Keiding 2006). As illustrated in Fig. 8, there was a slight tendency for higher K_1 estimates using whole-blood ^{13}N-concentration than ^{13}N-ammonia concentrations at low K_1 values, whereas the opposite was the case for high values of

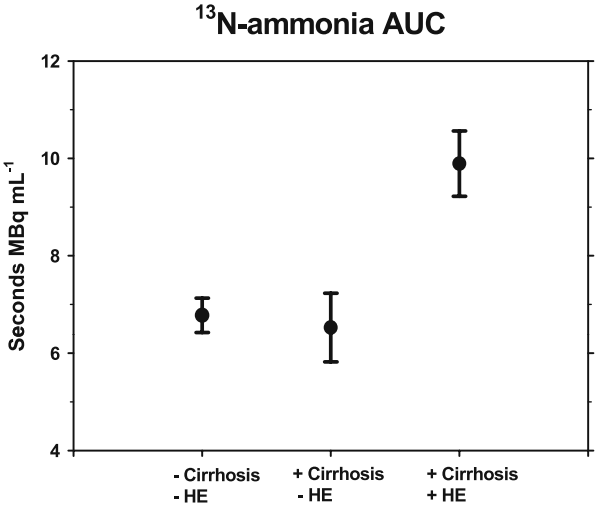

Fig. 6 Area under the curves (AUC) of blood concentrations of ^{13}N-ammonia in the groups of patients indicated (adapted from Sørensen and Keiding 2006). Since the same dose of ^{13}N-ammonia tracer was given to all subjects (500 MBq), the AUCs reflect "inverse" whole-body ammonia clearance estimates. Data are given as mean ± standard error of the mean

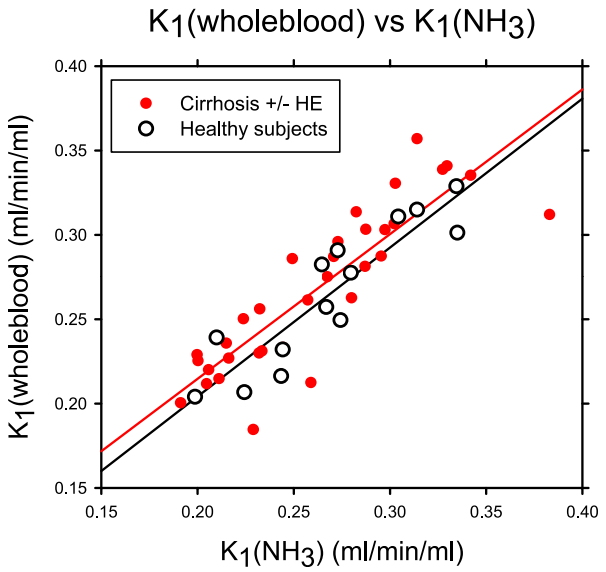

Fig. 8 Plot of the unidirectional clearance K_1 calculated from the model shown in Fig. 7, using either whole-blood ^{13}N-concentration (*Y-axis*) or ^{13}N-ammonia concentration (*X-axis*) as input function using the individual PET-data from the groups of patients indicated (adapted from Sørensen and Keiding 2006)

K_1. However, the difference from unity was not significant, and similarly there were no significant differences between healthy subjects and the two groups of patients with cirrhosis. Hence it is acceptable to use whole-blood ^{13}N-concentrations as input function for assessment of initial brain ammonia kinetics, including estimates of the blood-brain-barrier permeability for ammonia. In this connection it must be emphasized however, that the use of total ^{13}N-concentration as input function for calculation of parameters for metabolic processes during quasi steady-state such as for example the net metabolic clearance (K_{met}, Fig. 7) inevitably will yield incorrect results (Sørensen and Keiding 2006; Bass et al. 2009). The finding of a significant back-flux of ^{13}N-ammonia from brain to blood (Fig. 7) as quantified by $K_{met} < K_1$ in each of the subjects from Keiding et al. (2006) (Sørensen et al. 2009) would not have been possible without using ^{13}N-ammonia concentrations as input functions in the kinetic analyses.

Conclusion

Our fractionation of ^{13}N-content in blood is based on modification and duplication of the original sequential solid phase extraction procedure proposed by Rosenspire et al. (1990). Recent PET-studies of brain ammonia kinetics, using this procedure (Keiding et al. 2006) underline the importance of using ^{13}N-metabolite-corrected blood input curves for assessment of organ ammonia metabolism. The modified procedure thus enables analysis of enough blood samples to perform detailed kinetic analysis of dynamic ^{13}N-ammonia PET studies including steady-state ammonia metabolism in brain and liver.

The present analysis of the time courses of the ^{13}N-ammonia and ^{13}N-metabolite curves furthermore indicate that the metabolic conversion of ammonia took place in the order: healthy subjects > cirrhotic patients without HE > cirrhotic patients with HE.

Acknowledgements The study was supported by grants from the Novo Nordisk Foundation, the Danish Medical Research Council (271-08-0505), and the NIH (Grant 1 R01 DK074419-01).

References

Ahl B, Weissenborn K, van den Hoff J, Fischer-Wasels D, Kostler H, Hecker H, Burchert W (2004) Regional differences in cerebral blood flow and cerebral ammonia metabolism in patients with cirrhosis. Hepatology 40:73–79

Bass L, Keiding S, Munk OL (2009) Benefits and risks of transforming data from dynamic positron emission tomography, with an application to hepatic encephalopathy. J Theor Biol 256:632–636

Berding G, Banati RB, Buchert R, Chierichetti F, Grover VPB, Kato A, Keiding S, Taylor-Robinson SD (2009) Radiotracer Imaging studies in hepatic encephalopathy: ISHEN practice guidelines. Review. Liver Int 29:621–628

Berl S, Takagaki G, Clarke DD, Waelsch H (1962) Metabolic compartments in vivo. Ammonia and glutamic acid metabolism in brain and liver. J Biol Chem 237:2562–2569

Butterworth RF (2002) Pathophysiology of hepatic encephalopathy: A new look at ammonia. Metab Brain Dis 17:221–227

Cooper AJL (2001) Role of glutamine in cerebral nitrogen metabolism and ammonia neurotoxicity. Ment Retard Dev Disabil Res Rev 7:280–286

Cooper AJ, Plum F (1987) Biochemistry and physiology of brain ammonia. Physiol Rev 67:440–519

Cooper AJ, McDonald JM, Gelbard AS, Gledhill RF, Duffy TE (1979) The metabolic fate of ^{13}N-labeled ammonia in rat brain. J Biol Chem 254:4982–4992

Duda GD, Handler P (1958) Kinetics of ammonia metabolism in vivo. J Biol Chem 232:303–314

Hansen BA, Vilstrup H (1985) Increased intestinal hydrolysis of urea in patients with alcoholic cirrhosis. Scand J Gastroenterol 20:346–350

Iversen P, Sørensen M, Bak LK, Waagepetersen HS, Vafaee MS, Borghammer P, Mouridsen K, Jensen SB, Vilstrup H, Schousboe A, Ott P, Gjedde A, Keiding S (2009) Low cerebral oxygen consumption and blood flow in patients with cirrhosis and an acute episode of hepatic encephalopathy. Gastroenterology 136:863–871

Johansen ML, Bak LK, Schousboe A, Iversen P, Sørensen M, Keiding S, Vilstrup H, Gjedde A, Ott P, Waagepetersen HS (2007) The metabolic role of isoleucine in detoxification of ammonia in cultured mouse neurons and astrocytes. Neurochem Int 50:1042–1051

Jones EA, Basile AS (1998) Does ammonia contribute to increased GABA-ergic neurotransmission in liver failure? Metab Brain Dis 13:351–360

Keiding S, Munk OL, Roelsgaard K, Bender D, Bass L (2001) Positron emission tomography of hepatic first-pass metabolism of ammonia in pig. Eur J Nucl Med 28:1770–1775

Keiding S, Munk OL, Vilstrup H, Nielsen DT, Roelsgaard K, Bass L (2005) Hepatic microcirculation assessed by PET of first-pass ammonia metabolism in porcine liver. Liver Int 25:171–176

Keiding S, Sørensen M, Bender D, Munk OL, Ott P, Vilstrup H (2006) Brain metabolism of ^{13}N-ammonia during acute hepatic encephalopathy in cirrhosis measured by PET. Hepatology 43:42–50, Correction in Hepatology 2006; 44: 1056

Lockwood AH, McDonald JM, Reiman RE, Gelbard AS, Laughlin JS, Duffy TE, Plum F (1979) The dynamics of ammonia metabolism in man. Effects of liver disease and hyperammonemia. J Clin Invest 63:449–460

Lockwood AH, Bolomey L, Napoleon F (1984) Blood-brain barrier to ammonia in humans. J Cereb Blood Flow Metab 4:516–522

Lockwood AH, Yap EW, Wong WH (1991) Cerebral ammonia metabolism in patients with severe liver disease and minimal hepatic encephalopathy. J Cereb Blood Flow Metab 11:337–341

Mobley H, Hausinger RP (1989) Microbial ureases: significance, regulation and molecular characterization. Microbiol Rev 53:85–108

Nieves E, Rosenspire KC, Filc-DeRicco S, Gelbard AS, Cooper AJ (1986) High-performance liquid chromatographic on-line flow-through radioactivity detector system for analyzing amino acids

and metabolites labeled with nitrogen-13. J Chromatogr 383:325–337

Nishiguchi S, Shiomi S, Kawamura E, Ishizu H, Habu D, Torii K, Kawabe J (2003) Evaluation of ammonia metabolism in the skeletal muscles of patients with cirrhosis using N-13 ammonia PET. Ann Nucl Med 17:417–419

Prior RL, Visek J (1972) Effects of urea hydrolysis on tissue metabolite concentrations in rats. Am J Phys 223:1143–1149

Rosenspire KC, Schwaiger M, Mangner TJ, Hutchins GD, Sutorik A, Kuhl DE (1990) Metabolic fate of [^{13}N]ammonia in human and canine blood. J Nucl Med 31:163–167

Sørensen M, Keiding S (2006) Ammonia metabolism in cirrhosis. In D Häussinger, G Kircheis, F Schliess (eds.) Hepatic Encephalopathy and Nitrogen Metabolism, Springer pp 406−419

Sørensen M, Keiding S (2007a) New findings on cerebral ammonia uptake in HE using functional ^{13}N-ammonia PET. Metab Brain Dis 22:277–284

Sørensen M, Keiding S (2007b) Positron emission tomography of the liver. In: J Rodés, J-P Benhamou, A Blei, J Reichen, M Rizzetto (eds.) Textbook of Hepatology: From Basic Science to Clinical Practice. 3. ed. Blackwell Publishing pp 561–566

Sørensen M, Munk OL, Keiding S (2009) Backflux of ammonia from brain to blood in human subjects with and without hepatic encephalopathy. Metab Brain Dis 24:237–242

Weissenborn K, Bokemeyer M, Ahl B, Fischer-Wasels D, Giewekemeyer K, van den Hoff J, Köstler H, Berding G (2004) Functional imaging of the brain in patients with liver cirrhosis. Metab Brain Dis 19:269–280